Original Article

progress in Reaction Kinetics and Mechanism

Progress in Reaction Kinetics and Mechanism
Volume 46: 1–13
© The Author(s) 2021
Article reuse guidelines:
sagepub.com/journals-permissions
DOI: 10.1177/1468678320956864
journals.sagepub.com/home/prk
SAGE

Three-component reaction involving isoquinoline and dimethyl acethylenedicarboxylate in the presence of indole: Theoretical and experimental investigations of the reaction mechanism

Mohammad Zakarianezhad[1], Sayyed Mostafa Habibi-Khorassani[2], Batoul Makiabadi[3] and Elham Zeydabadi[1]

Abstract

The reaction kinetics among isoquinoline, dimethyl acetylenedicarboxylate, and indole (as NH-acid) were investigated using ultraviolet (UV) spectrophotometry. The reaction rate equation was obtained, the dependence of the reaction rate on different reactants was determined, and the overall rate constant (k_{ov}) was calculated. By studying the effects of solvent, temperature, and concentration on the reaction rate, some useful information was obtained. A logical mechanism consistent with the experimental observations was proposed. Also, comprehensive theoretical studies were performed to evaluate the potential energy surfaces of all structures that participated in the reaction mechanism. Finally, the proposed mechanism was confirmed by the obtained results and the probable and logical reaction paths and also a correct product configuration were suggested based on the theoretical results.

Keywords

NH-acid, ultraviolet spectrophotometry, isoquinoline, kinetic parameters, acetylenic ester, theoretical study

[1]Department of Chemistry, Payame Noor University, Tehran, Iran
[2]Department of Chemistry, University of Sistan and Baluchestan, Zahedan, Iran
[3]Department of Chemical Engineering, Sirjan University of Technology, Sirjan, Iran

Corresponding author:
Mohammad Zakarianezhad, Department of Chemistry, Payame Noor University of Sirjan, Sirjan, P.O. Box 78157, Iran.
Email: m.zakarianejad@yahoo.com; mzakarianejad@pnu.ac.ir

Creative Commons Non Commercial CC BY-NC: This article is distributed under the terms of the Creative Commons Attribution-NonCommercial 4.0 License (https://creativecommons.org/licenses/by-nc/4.0/) which permits non-commercial use, reproduction and distribution of the work without further permission provided the original work is attributed as specified on the SAGE and Open Access pages (https://us.sagepub.com/en-us/nam/open-access-at-sage).

Introduction

Multicomponent reactions (MCRs) have been recognized as strong tools in modern drug discovery procedure since these types of reactions make it easy and rapid to access the structural variation and complexity of compounds through single-step conversions.[1,2] Such reactions are rapid, well-diversified, efficient, atom-economic, and environment-friendly.[3,4] Due to the advantages mentioned above, developing new MCRs with environmentally benign protocols has been recognized as one of the most important topics in synthetic chemistry.[5–7] MCRs display many of the most desired features for an organic synthesis,[8–10] and they have been intensively studied in recent years.[11–14] Heterocyclic rings are the fundamental components in the skeleton of more than half of the biologically active compounds produced by nature.[15] As an example, aza-aromatic compounds that are activated by acyl chlorides or dimethyl acetylenedicarboxylate (DMAD) are important intermediates for the synthesis of a variety of biologically active nitrogen-containing alkaloids.[16,17] This is why great efforts have been made to discover and optimize methods to construct new heterocycles.

Isoquinoline skeleton can be found in a large number of naturally occurring[18–21] and biologically synthesized active heterocyclic compounds.[22,23] In particular, 1,2-dihydroisoquinoline derivatives act as delivery systems that transport drugs through the highly impermeable blood−brain barrier.[24,25] These compounds also exhibit sedative,[26] antidepressants,[27] antitumor, and antimicrobial activities.[28,29] With wide kinetic studies been done in the synthesis of phosphorus ylides,[30–34] the structural effect of the reactant (different NH-acids and dialkyl acetylenedicarboxylates) on the reaction rate has been well investigated. Changes in the reactant structure that participates in the reaction, eventuates changes in the overall reaction rate. Evaluating these changes could reveal many facts about the confirmation of the reaction mechanism. A number of our projects, including the theoretical and experimental studies of chemical reaction kinetics, have been completed.[35–41] Now, by the synthesis of the novel compounds via a pseudo-three-component reaction, in the presence of isoquinoline **1**, DMAD **2,** and different NH-acids **3**,[42] an opportunity has been achieved to investigate the effect of changing the structure of the first component participating in the reaction (i.e. isoquinoline instead of triphenylphosphine) along with the effect of changing the structure of the NH-acids on the kinetic parameters and reaction mechanism. Using available information and based on well-established chemistry of trivalent phosphorus and nitrogen nucleophiles,[43–46] it is reasonable that the product results from initially adding the isoquinoline to DMAD (**2**) and subsequent protonation of the 1:1 adduct by the NH-acid **3** to form the product (Figure 1). To gain further insight into the reaction mechanism, a kinetic study, including determining the preferred kinetic path, investigation of intermediate structures and transition states in the reaction path, determination of the kinetic and thermodynamic stabilities of products, recognition of rate-determining step, calculation of the reaction rate and finally, identifying and confirming the reaction mechanism are the issues that have been first explored for this class of reactions using ultraviolet (UV) spectrophotometry. Also, another goal of this project was to investigate the effect of substituted groups on the structure of NH-acid. Therefore, to investigate the effect of the substituted methyl group as an electron donor group, the results of this study will be compared with the results obtained in the presence of NH-acid 3-methyl indole[36] and will be examined.

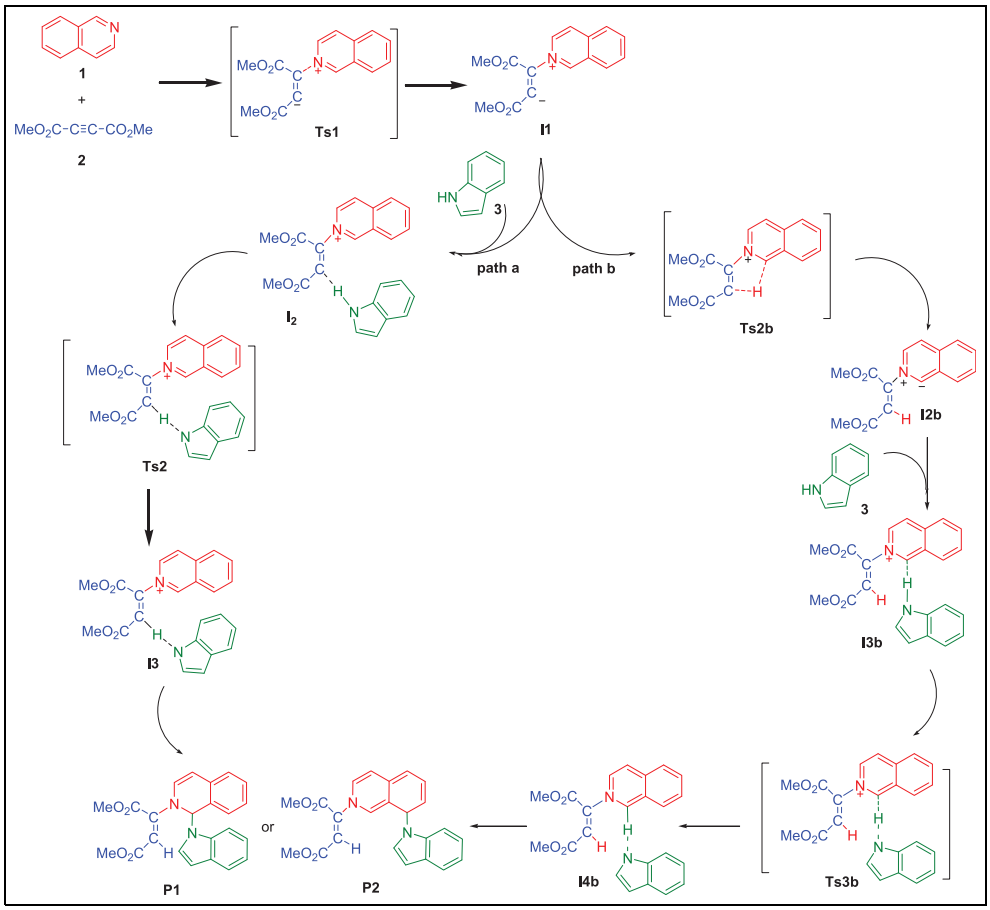

Figure 1. The reaction among isoquinoline **1**, dimethyl acetylenedicarboxylate **2,** and indole **3** for the synthesis of N-amino esters.

Materials and methods

DMAD, isoquinoline, and indole, purchased from Fluka (Buchs, Switzerland), were used without further purifications. All the other pure solvents including dichloromethane and acetone were purchased from Merck (Darmstadt, Germany). A Cary UV/Vis spectrophotometer model Bio-300 (Australia) was also applied throughout this work. All geometrical structures were optimized at B3LYP/6-311++G (2d, 2p) level of theory using the Gamess suite software package.[47] The corresponding frequencies of the structures were estimated at the same level of theory to check the stationary points without imaginary frequencies and the transition states with only one imaginary frequency. Also, the intrinsic reaction coordinate (IRC) approach[48,49] was followed to ensure that the given transition state is related to the corresponding reactants and products. The solvent effect on complex stability was examined using the B3LYP/6-311++G (2d, 2p) method by applying the polarizable continuum model (PCM).

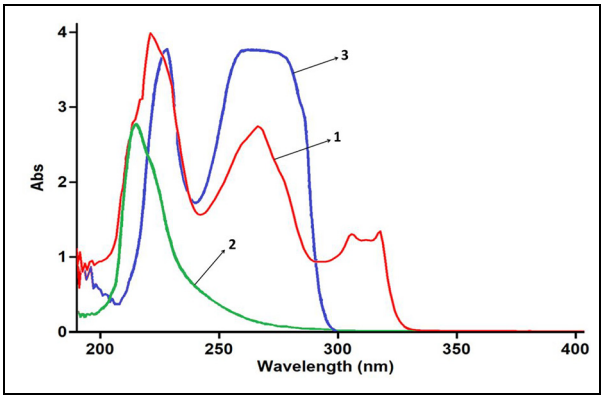

Figure 2. The plot of absorbance versus wavelength of the solution 3-mM isoquinoline **1** (red line), dimethyl acetylene-dicarboxylate **2** (green line), and indole **3** (blue line) in dichloromethane.

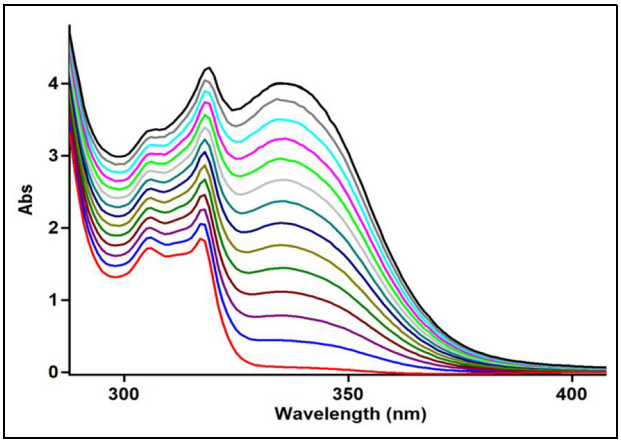

Figure 3. Expanded section of UV spectra (an increasing absorption) over the wavelength range 280–400 nm for the reaction among **1** (30 mM), **2** (3 mM), and **3** (3 mM) in dichloromethane.

Results and discussion

Experimental studies

The first step in investigating the reaction kinetics is to determine the appropriate wavelength. So, for this purpose, the UV spectra of 3-mM dichloromethane solution of compounds **1**−**3** were recorded separately over the wavelength range of 190–400 nm (Figure 2). In the second step, the UV spectrum was recorded for the reaction among a higher concentration of **1** (30 mM) with **2** and **3**, every 25 min (Figure 3). A comparison of the results obtained in Figures 1 and 2 shows that the spectrum recorded in the range of 330–380 nm is part of the product **4** spectrum where the reactant lacks any absorption spectrum. It should be noted that a specific concentration of reactants must be used, which provides a normal

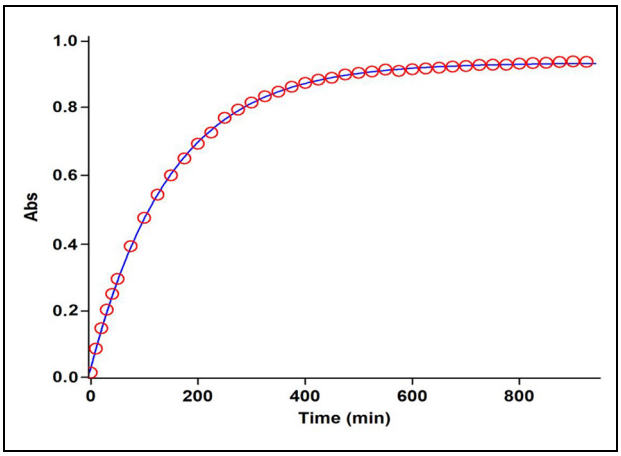

Figure 4. The experimental absorbance changes (dotted line) versus time accompanied by the second-order fit curve (solid line) for the reaction among **1** (30 mM), **2** (3 mM), and **3** (3 mM) at 15.0°C and 370 nm in dichloromethane.

absorption of the product (0.8–1.2) in the wavelength range of 330–380 nm. Selecting 370 nm in the wavelength range of 330–380 nm, which has a good absorption value (0.9), would be a suitable choice for kinetic measurements.

The reaction kinetics were then followed by plotting UV absorbance versus time for the reaction among **1** (30 mM), **2** (3 mM), and **3** (3 mM) at 15.0°C. The time dependency of this absorbance is represented in Figure 4. The absorbance at reaction completing time (A_∞) can be obtained from this plot at $t = 950$ min. Under this condition, the rate equation can be expressed as

$$\text{Rate} = k_{\text{obs}}[2]^{\beta}[3]^{\gamma} \text{and } k_{\text{obs}} = k_{\text{ov}}[1]^{\alpha} \tag{1}$$

Using nonlinear regression analysis,[50] the data of original experimental absorbance versus time provided a pseudo-first-order curve (solid line) that exactly coincides with the experimental curve (dotted line), as shown in Figure 4. The pseudo-first-order rate constant (k_{obs}) was also calculated at 15.0°C. The observed pseudo-first-order rate constant (k_{obs}) indicates that the order of reaction concerning the sum of compounds **2** and **3** is equal to one ($\beta + \gamma = 1$).

Continuing the experiments, the reaction among **1** (3 mM), **2** (30 mM), and **3** (3 mM) at 15.0°C was conducted, in which the rate equation can be expressed as

$$\text{Rate} = k'_{obs}[1]^{\alpha}[3]^{\gamma} \text{and } k'_{obs} = k_{\text{ov}}[2]^{\beta} \tag{2}$$

The data of original experimental absorbance versus time were used to provide a pseudo-first order fit curve (solid line) at 370 nm, which exactly coincides with the experimental curve (dotted line). In this case, the observed pseudo-first order rate constant (k'_{obs}) indicates that the order of reaction concerning the sum of compounds **1** and **3** ($\alpha + \gamma = 1$) is equal to one. Given ($\beta + \gamma = 1$) and ($\alpha + \gamma = 1$), it is obvious that $\gamma = 0$ and the order of the

Table 1. Values of the overall second-order rate constant (k_2) for the reactions of **1–3** in the presence of solvents such as dichloromethane and acetone, respectively, at all temperatures, investigated.

Solvent	k_2/M^{-1} min^{-1}			
	15.0°C	20.0°C	25.0°C	30.0°C
Dichloromethane	5.5 ± 0.1	8.4 ± 0.2	12.2 ± 0.4	17.8 ± 0.4
Acetone	6.4 ± 0.1	9.0 ± 0.3	13.3 ± 0.2	19.1 ± 0.3

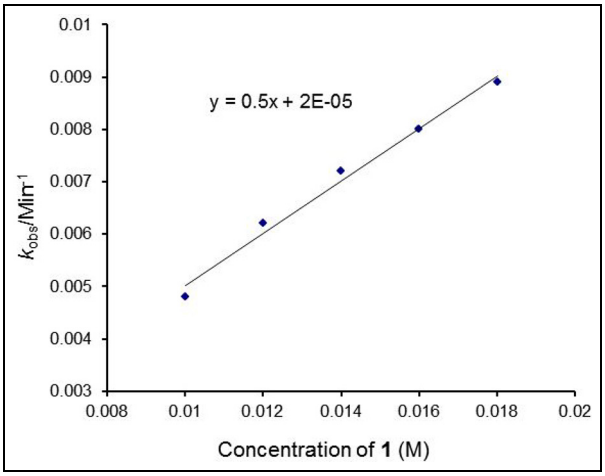

Figure 5. Observed rate constant (k_{obs}) versus concentration of reactant **1** at 370 nm and 15.0°C in dichloromethane. [1] = 3×10^{-2}–5.4×10^{-2} M and [2] = [3] = 3×10^{-3} M.

reaction with respect to indole **3** is equal to zero. The above results show that the overall reaction order is equal to two ($\alpha + \beta + \gamma = 2$).

To further confirm the above results, all kinetics were studied in the presence of isoquinoline **1** at different concentrations (ranging from 3.6×10^{-2} to 5.4×10^{-2} M) with a constant concentration of **2** and **3** (3 mM). The straight line obtained from the plot of observed pseudo-first-order rate constant (k_{obs}) versus [1] (Figure 5) proved that the reaction is of first-order concerning compound **1** ($\alpha = 1$). The overall rate constant (k_{ov}) was calculated based on the slope of the line in Figure 5 and was reported in Table 1. The same results obtained in the presence of DMAD **2** at different concentrations (ranging from 3.6×10^{-2} to 5.4×10^{-2} M) indicating the reaction is of first-order to the compound **2** ($\beta = 1$). As a result, since ($\beta + \gamma = 1$) and ($\alpha + \gamma = 1$) (as determined previously), it is obvious that $\gamma = 0$ and order of reaction to indole **3** must be equal to zero. All the above results indicate that the overall reaction order is equal to two ($\alpha + \beta + \gamma = 2$).

To determine the effects of temperature and solvent environment on the reaction rate, a set of experiments was conducted at different temperatures and solvent polarities with other conditions being the same as those of the previous experiments. For this purpose, acetone, with the dielectric constant of 20.7 was replaced by dichloromethane with a dielectric

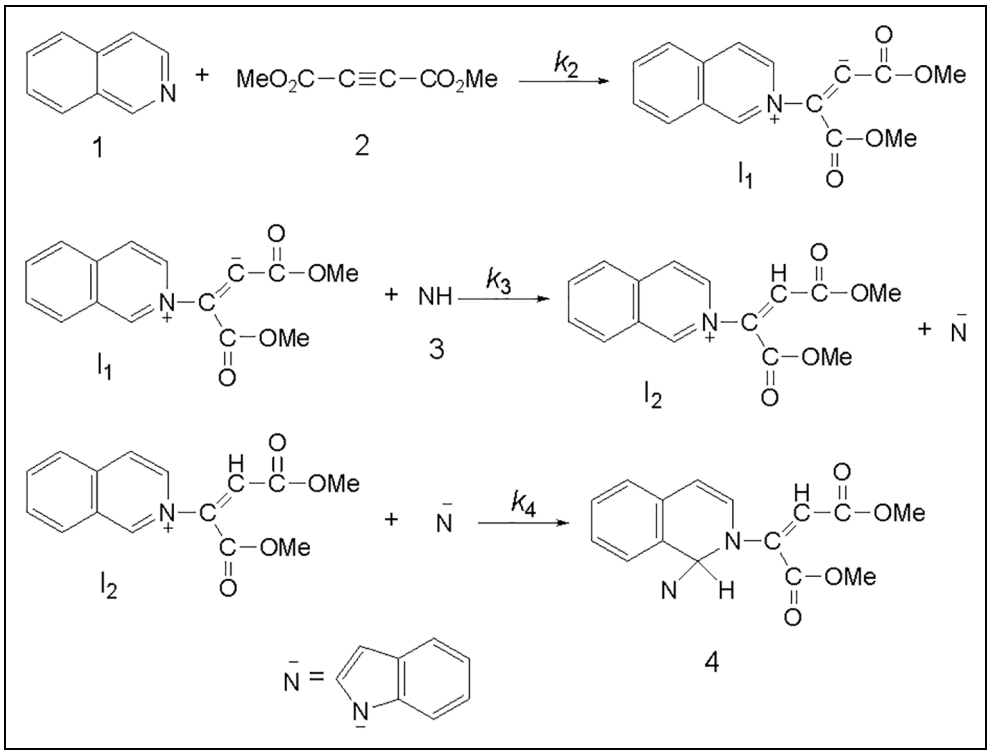

Figure 6. Proposed mechanism for the reaction among **1, 2,** and **3** for the generation of N-amino esters **4**.

constant of 8.9. Based on the results, the rate of reaction was accelerated in an environment with a higher dielectric constant (acetone). Also, at all the investigated temperatures, the results indicate an increase in reaction rates at higher temperatures (Table 1). In the studied range of temperatures, the reaction activation energy was calculated from the slope of the pseudo-second-order rate constant ($\log k_{ov}$) versus reciprocal temperature ($1/T$).

Rate equation. Based on the above results, a simplified proposed reaction mechanism is depicted in Figure 6. Unlike the experimental results, it may be assumed that the second step is the rate-determining step for the proposed mechanism. In this case, the rate equation can be expressed as follows

$$\text{Rate} = \frac{k_2 k_3 [1][2][3]}{k_{-2}} \tag{3}$$

The final equation indicates that the overall order of the reaction is three which is not compatible with experimental overall order of reaction (= 2). Besides, according to this equation, the order of reaction to indole **3** is one, whereas it was shown to be equal to zero. For this reason, it appeared that the second step is fast.

If we assume that the third step (rate constant k_4) is the rate-determining step for the proposed mechanism, in this case, there are two ionic species to consider in the rate-determining

Table 2. Activation parameters for the reactions **1–3**.

Solvent	Ea (kJ mol^{-1})	$\Delta H^{\#}$ (kJ mol^{-1})	$\Delta S^{\#}$ (J mol^{-1} K^{-1})	$\Delta G^{\#}$ (kJ mol^{-1})
Dichloromethane	56.6 ± 2.3	54.2 ± 2.2	–76.5 ± 2.8	76.8 ± 2.7
Acetone	53.3 ± 1.8	50.8 ± 1.8	–86.9 ± 2.7	76.5 ± 2.6

step (I2 and N^-) (Figure 6), have full positive and negative charges and form very powerful ion–dipole bonds to the acetone as a higher dielectric constant solvent. However, the transition state for the reaction between two ions carries a dispersed charge and bonding of solvent (acetone) to this dispersed charge would be much weaker than the reactants. The solvent, thus stabilizes the ionic species, more than it would the transition state. Therefore, the activation energy could be raised and slow down the reaction. However, in practice, acetone speeds up the reaction and for this reason, the third step could not be the rate-determining step. Furthermore, the rate law can be expressed as

$$\text{Rate} = k_2\ k_3\ k_4\ [1]\ [2]\ [3] \tag{4}$$

The final equation also indicates that the overall order of the reaction is three, and the order of reaction for indole **3** is one, which is not compatible with experimental results.

If the first step (rate constant k_2) was the rate-determining step, in this case, bonding of solvent to the dispersed charge in the transition state is much stronger than the uncharged reactants. The solvent thus stabilizes the transition state more than it does the reactants and speeds up the reaction. Our experimental results show that the solvent with higher dielectric constant exerts a powerful effect on the rate of reaction (see Table 1). Results indicate that the first step (k_2) of the proposed mechanism could be the rate-determining step. However, a good kinetic description of the experimental result using a mechanistic scheme based upon the steady-state approximation is frequently taken as an evidence of its validity. By application of this, the rate of the formation of product **4** from the reaction mechanism (Figure 6) is given by

$$\frac{d[4]}{dt} = \frac{d[\text{product}]}{dt} = \text{rate} = k_4[I_2][N^-] \tag{5}$$

By replacing the value of [I1] and [I2]

$$\text{Rate} = k_2[1][2] \tag{6}$$

This equation is compatible with the results obtained by UV spectrophotometry. For equation (6) that shows the overall reaction rate, the activation parameters involving $\Delta G^{\#}$, $\Delta S^{\#}$, and $\Delta H^{\#}$ could be now calculated for the first step (rate-determining step), as an elementary reaction, based on Eyring equation. The results are reported in Table 2.

The activation parameters ($\Delta G^{\#}$, $\Delta S^{\#}$, and $\Delta H^{\#}$) of the first step (rate-determining step), as an elementary reaction, can be calculated based on the Eyring equation. The results are reported in Table 2.

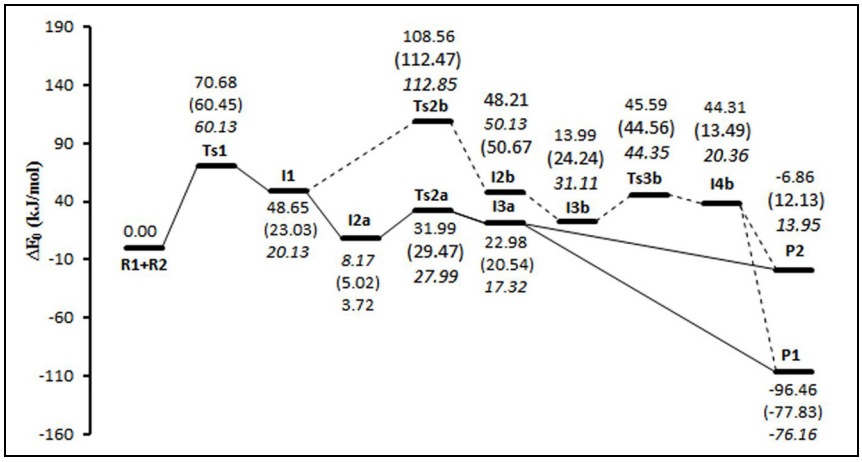

Figure 7. The potential energy profile of the reaction in paths **a** and **b** (data of dichloromethane are in parentheses and data of acetone are in italic form).

Theoretical study

The overall order of reaction and the order of reaction to different reactants, solvent, and temperature effect and also the detection of rate-determining step, and finally, the reaction mechanism as well are determined in the experimental section. Now, to gain more insight into the reaction mechanism, we intend to consider the mechanism of this reaction using theoretical calculations.

In this section, we will evaluate the potential energy levels, different kinetic paths, and energy levels of different products. Also, we intend to determine the preferred thermodynamic product, the kinetic preferred path, and to confirm the rate-determining step, as outlined in the experimental section. All structures were optimized by density functional theory at B3LYP/6-311++G (2d, 2p) level of theory. Two different pathways (**a** and **b**) were predicted for this reaction. Potential energy profiles for the pathways **a** and **b** are presented in Figure 7. Also, the optimized geometries of all structures are presented in Figure 8. As can be seen, the reaction path **b** includes four steps. The first step initiates with a nucleophilic attack of atom N17 in the structure of isoquinoline (**R2**) to atom C8 of DMAD (**R1**) to form **I1**, via passing through **Ts1**. The second step includes an intramolecular proton transfer from atom C32 to atom C9, via **Ts2b**, to form **I2b**. Then, **I3b** structure can be formed by the hydrogen bonding interaction of **I2b** and **R3**. The third step includes an intermolecular proton transfer from atom N34 of indole (**R3**) to atom C32 in the structure of **Ts3b**, to form **I4b**. In the fourth step, once the indole ion attacks atoms C18 or C21, stable products, **P1** and **P2** are formed, respectively. The fourth step proceeds without any activation barrier. This result seems to be due to the high tendency of indole ion for bonding to C18 or C21. The two pathways, **a** and **b,** also lead to the formation of identical products. The path **a** includes three steps with the first step being the same as that of the path **b** and the second step including a direct intermolecular proton transfer from atom N34 in indole (**R3**) to atom C9 within the structure of **Ts2a**, to form **I3a**. The very high tendency of the indole ion towards forming

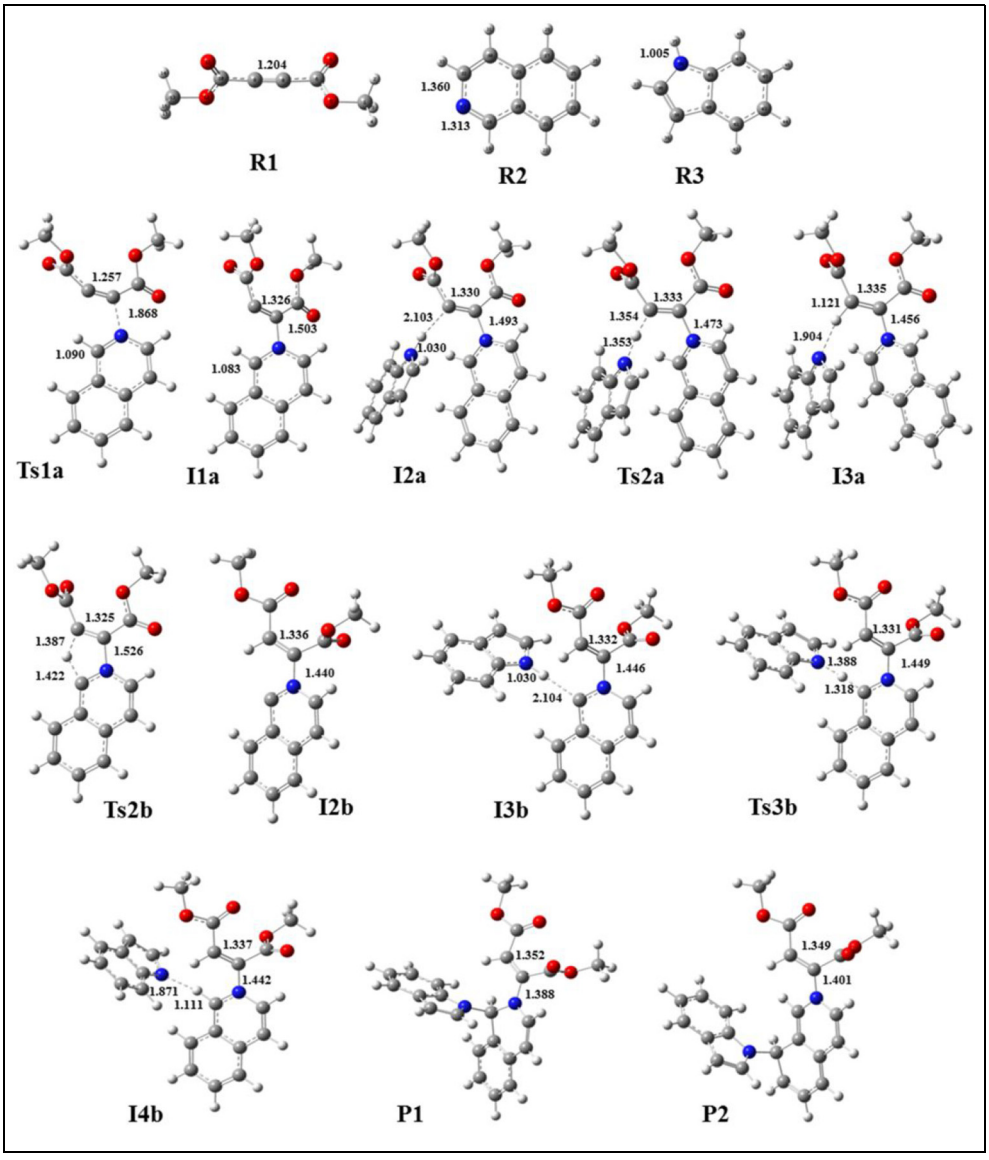

Figure 8. Optimized geometries of all structures in pathways **a** and **b** of the reaction accompanied by geometrical parameters.

N34-C18 or N34-C21 bonds caused the third step of the reaction to proceed without producing any activation barrier, as same as the path **b**.

Investigation of the potential energy surfaces in the pathways **a** and **b** shows that the first step of the two pathways **a** and **b** with an energy barrier of 70.68 kJ/mol was recognized as the rate-determining step. Because this step of the reaction is a common step for two kinetic paths **a** and **b**, no kinetic preference was observed in these pathways. Also, because both

kinetic paths lead to the same products (**P1** or **P2**), no thermodynamic preference was observed. Despite these, the path **a**, because of less exhausted energy, is more preferable. In addition to the experimental results which imply the absence of the product **P2**, theoretical studies also show that the product **P2** is considerably more unstable than **P1**, by the value of 103.32 kJ/mol, which can be a factor in the absence of this product.[42] Also, the geometrical structures in Figure 8 show that C18 is more accessible for nucleophilic attack in the last step of the reaction.

To check the effect of solvent on the potential energy surfaces, dichloromethane was subjected to condensed phase calculations carried out using the PCM. As shown in Figure 6, the energy barrier of the first and the third step of the pathway **b** has decreased, but that of the second step considerably increased, both in dichloromethane and acetone. In this condition, the second step of the reaction is determined to be the rate-determining step which is in contrast to what was obtained in the experimental section and the gas phase. Both energy barriers of the pathway **a** decreased and results show that the first step of the reaction is determined to be the rate-determining step. Results indicate that pathway **a** has a considerable kinetic preference rather than that of **b**. Also, the only path is compatible with the increasing of the reaction rate with increasing of dielectric constant of the solvent in experimental results. Similar results were obtained from theoretical investigations. The product **P2** is more unstable than the **P1,** both in dichloromethane and acetone, by the value of 89.96 and 90.11 kJ/mol, respectively and it suggests that products **P2** cannot exist. Although the calculations in the gas phase do not show any superiority between the two paths, but in the solution phase, the path **a** is preferable because of the matching with experimental results and kinetic superiority to path **b**. Theoretical results illustrate how the first step of the reaction is the rate-determining step and show the effect of solvents with higher dielectric constant in reducing the energy barrier of this reaction.

Conclusion

Mechanistic investigation of the reaction among isoquinoline **1**, DMAD **2** in the presence of NH-acid, such as indole **3** was investigated both experimentally and theoretically. The results are summarized below.

The kinetics of the reaction were studied by measuring the increase in the product absorption rate. The overall reaction order follows the pseudo-second-order kinetics with the first-order dependent on the concentration of isoquinoline **1** and DMAD **2**. The reaction activation parameters were calculated by measuring the rate constant at different temperatures. Recognizing the first step of the reaction (k_1) as the rate-determining step, a mechanism was proposed for the reaction based upon experimental and theoretical results. For all reactions, the rates were increased by increasing the dielectric constant of the solvent. The effect of temperature on the reaction rate is much more than that of the solvent dielectric. The computational results in solution do not show any thermodynamic priority between the two studied kinetic pathways, but the pathway **a**, because of the more kinetic preference, is more preferable than the pathway **b**. Comparing the results obtained in this project with the results obtained in our previous project in the presence of isoquinoline **1,** DMAD **2,** and 3-methyl indole **3**[36] shows that as expected, the reaction in the presence of the methyl electron donor group has more activation energy. The electron donor groups reduce the acidic strength of NH-acid. Therefore, it has slowed down the overall reaction rate.

Declaration of conflicting interests

The author(s) declared no potential conflicts of interest with respect to the research, authorship, and/or publication of this article.

Funding

The author(s) disclosed receipt of the following financial support for the research, authorship, and/or publication of this article: The authors sincerely thank Payame Noor University for providing financial support for this work.

References

1. Dömling A. *Chem Rev* 2006; 106: 17–89.
2. Lieby-Muller F, Constantieux T and Rodriguez J. *J Am Chem Soc* 2005; 127: 17176–17177.
3. Pando O, Stark S, Dankert A, et al. *J Am Chem Soc* 2011; 133: 7692–7695.
4. Shaabani A, Rezayan AH, Keshipour S, et al. *Org Lett* 2009; 11: 3342–3345.
5. Ganem B. *Acc Chem Res* 2009; 42: 463–472.
6. Candeias NR, Veiros LF, Carlos AM, et al. *Eur J Org Chem* 2009; 12: 1859–1863.
7. Ning M, Jiang B, Zhang G, et al. *Green Chem* 2010; 12: 357–1361.
8. Wender PA, Haddy ST and Wright DL. *Chem Ind* 1997; 765: 767–769.
9. Maghsoodlou MT, Habibi-Khorassani SM, Rofouei K, et al. *Arkivoc* 2006; xii: 145–151.
10. Dastoorani P, Khalilzadeh MA, Khaleghi F, et al. *New J Chem* 2019; 43: 6615–6621
11. Ugi I, Dömling A and Werner B. *J Heterocyclic Chem* 2000; 37: 647–658.
12. Yavari I, Anary-Abbasinejad M and Monatshefte AA. *Fur Chemie* 2002; 133: 1331–1336.
13. Adib M, Yavari H and Mollahosseini M. *Tetrahedron Lett* 2004; 45: 1803–1805.
14. Nair V, Sreekanth AR, Abhilash N, et al. *Synthesis* 2003; 12: 1895–1902.
15. Katritzky AR and Rees CW. *Comprehensive heterocyclic*. New York: Pergamon Press, 1984.
16. Yavari I, Hossaini Z, Sabbaghan M, et al. *Tetrahedron* 2007; 63: 9423–9428.
17. Nair V, Devipriya S and Eringathodi S. *Tetrahedron Lett* 2007; 48: 3667.
18. Díaz JL, Miguel M and Lavilla R. *J Org Chem* 2004; 69: 3550–3553.
19. Adib M, Mollahosseini M, Yavari H, et al. *Synthesis* 2004; 06: 861–864.
20. Yavari I, Hossaini Z and Sabbaghan M. *Tetrahedron Lett* 2006; 47: 6037–6040.
21. Gilchrist TL. *Heterocyclic chemistry*. New York: Wiley, 1985.
22. Michael JP. *Nat Prod Rep* 2002; 19: 742–760.
23. Scott JD and Williams RM. *Chem Rev* 2002; 102: 1669–1730.
24. Sheha MM, El-Koussi NA and Farag H. *Arch Pharm* 2003; 336: 47–52.
25. Mahmoud S, Aboul-Fadl T, Shehq M, et al. *Arch Pharm* 2003; 336: 573–584.
26. Lukevics E, Segal I, Zablotskaya A, et al. *Molecules* 1997; 2: 180–185.
27. Maryanoff BE, McComsey DF, Gardocki JF, et al. *J Med Chem* 1987; 30:1433–1454.
28. Tietze LF, Rackehmann N and Miller I. *Chem Eur J* 2004; 10: 2722–2731.
29. Knölker HJ and Agarwal S. *Tetrahedron Lett* 2005; 46: 1173–1175.
30. Habibi-Khorassani SM, Maghsoodlou MT, Ebrahimi A, et al. *J Solution Chem* 2007; 36: 1117–1127.
31. Habibi-Khorassani SM, Ebrahimi A, Maghsoodlou MT, et al. *Curr Org Chem* 2011; 15: 942–952.
32. Habibi Khorassani SM, Maghsoodlou MT, Ebrahimi A, et al. *Prog React Kinet Mech* 2005; 30: 127–143.
33. Habibi-Khorassani SM, Maghsoodlou MT, Zakarianezhad M, et al. *Heteroat Chem* 2008; 19: 723–732.
34. Zakarianezhad M, Habibi-Khorassani SM, Ebrahimi A, et al. *Heteroat Chem* 2010; 21: 462–474.

35. Zakarianezhad M, Makiabadi B, Habibi-Khorassani SM, et al. *Res Chem Intermed* 2018; 44: 2653–2665.
36. Zakarianezhad M, Masoodi HR, Shool M, et al. *Int J Chem Kinet* 2016; 48: 770–778.
37. Zakarianezhad M and Shool M. *Iran Chem Commun* 2017; 5: 301–307.
38. Zakarianezhad M and Mohammadi L. *Phys Chem Res* 2016; 4: 221–230.
39. Zakarianezhad M, Masoodi HR and Shool M. *Phosp Sulf Silicon* 2016; 19: 1063–1069.
40. Zakarianezhad M and Mohammaddadi P. *J Sulf Chem* 2015; 36: 422–433.
41. Mohtat B, Siadati SA and Khalilzadeh MA. *Prog React Kinet Mech* 2019, 44: 213–221.
42. Nassiri M, Maghsoodlou MT, Heydari R, et al. *Mol Divers* 2008; 12: 111–117.
43. Cadogan JIG. *Organophosphorus reagents in organic synthesis*. New York: Academic Press, 1979.
44. Engel R. *Synthesis of carbon-phosphors bonds*. Boca Raton, FL: CRC Press, 1988.
45. Hudson HR. The chemistry of organophosphorus compounds. In: Hartley FR (ed.) *Primary, secondary and tertiary phosphates and heterocyclic organophosphorus (III) compounds*. New York: Wiley, 1990.
46. Corbridge DEC. *Phosphorus: An outline of chemistry, biochemistry, and uses*. Amsterdam: Elsevier, 1995.
47. Frisch MJ, Trucks GW, Schlegel HB, et al. *GAUSSIAN 09*. Pittsburgh, PA: Gaussian Inc., 2009.
48. Schmidt MW, Baldridge K., Boatz JA, Elbert ST, Gordon MS, Jensen JH, Koseki S, Matsunaga N, Nguyen KA, Su S, Windus TL, Dupuis M, Montgomery JA. *J Comput Chem* 1993; 14: 1347–1363.
49. Gonzalez C and Schlegel HB. *J Phys Chem* 1990; 94: 5523–5527.
50. Schwartz LM and Gelb RI. *Anal Chem* 1978; 50: 1592–1594.